DOI: 10.1002/chem.200701269

Highly Effective Acyclic Carbohydrate Receptors Consisting of Aminopyridine, Imidazole, and Indole Recognition Units

Monika Mazik* and Matthias Kuschel[a]

Abstract: Neutral imidazole/aminopyridine- and indole/aminopyridine-based receptors, **1** and **2**, have been established as highly effective and selective carbohydrate receptors. These receptors effectively recognise neutral carbohydrates through multiple interactions, including neutral hydrogen bonds and CH···π interactions between the sugar CH groups and the aromatic rings of the receptors. The design of these receptors was inspired by the binding motifs observed in the crystal structures of protein–carbohydrate complexes. The formation of very strong complexes with β-glucopyranoside **5**, β-maltoside **8**, and α-maltoside **9** in organic media has been characterised by ^{1}H NMR spectroscopy and confirmed by a second, independent technique, namely fluorescence spectroscopy. The syntheses, molecular-modelling studies, binding properties of the receptors **1** and **2** toward selected mono- and disaccharides as well as comparative binding studies with receptors **3** and **4** are described.

Keywords: carbohydrates · hydrogen bonds · molecular recognition · receptors · supramolecular chemistry

Introduction

Natural carbohydrate recognition is mediated by various classes of protein, such as lectins (the most intensively studied class), bacterial periplasmic proteins and antibodies. A number of interactions contribute to the stabilisation of protein–carbohydrate complexes, including neutral and ionic hydrogen bonds, metal coordination and packing of aromatic side chains against the sugar rings.[1] In the case of lectins and bacterial periplasmic proteins, most of the hydrogen bonds involve amino acid side-chain groups of the protein,[1a,f,g,h] such as amide (Asn, Gln), carboxylate (Asp, Glu), quanidinium (Arg), ammonium (Lys), hydroxy (Ser, Thr, Tyr), imidazole (His), and indole (Trp) groups (for examples of hydrogen-bonding interactions involving the imidazole or indole group, see Figure 1a, b and c). Main-chain amides also contribute to hydrogen bonding, but to a lesser extent[1h] (in contrast with antibodies, which seem to make greater use of main-chain amides[1j]). Packing of an aromatic ring of the protein, such as the indole of tryptophan or the phenyl ring of phenylalanine (see Figure 1d), against the sugar is observed in most carbohydrate-binding proteins.

The interactions observed in the crystal structures of protein–carbohydrate complexes inspire the development of different artificial receptor structures for the recognition of carbohydrates.[2–5] Our previous studies showed that acyclic receptors containing two to four recognition units interconnected by a phenyl, biphenyl or diphenylmethane spacer perform effective recognition of carbohydrates through multiple interactions.[3b–d,g–j,s,t,4k,s,t] Depending on the nature and number of recognition subunits and connecting bridges used as the building blocks, a variety of structures with different binding properties could be obtained (for examples of recognition and spacer units used for the construction of the acyclic receptors, see Scheme 1; for examples of binding motifs found in the receptor–sugar complexes, see Figure 2). The acyclic scaffold of the receptors provides simplicity in the synthetic plan for many modifications of the receptor structure, supplying a base for systematic studies toward recognition motifs for carbohydrates.

Herein, we describe the synthesis and binding properties of new carbohydrate receptors containing a 4(5)-substituted imidazole or a 3-substituted indole ring (receptors **1** and **2**,

[a] Prof. Dr. M. Mazik, Dipl.-Chem. M. Kuschel
Institut für Organische Chemie
der Technischen Universität Braunschweig
Hagenring 30, 38106 Braunschweig (Germany)
Fax: (+49) 5313-9181-85
E-mail: m.mazik@tu-bs.de

Supporting information for this article is available on the WWW under http://www.chemeurj.org/ or from the author and contains ^{1}H und ^{13}C NMR spectra of compounds **1**–**4**, IR data of compounds **1**–**4**, examples of ^{1}H NMR titrations of receptor **3** and **4** with β-glucopyranoside **5**, an example of ^{1}H NMR titration of β-glucopyranoside **5** with receptor **3** (inverse titration), further examples of titration curves, representative mole-ratio plots and X-ray data for compound **11.**

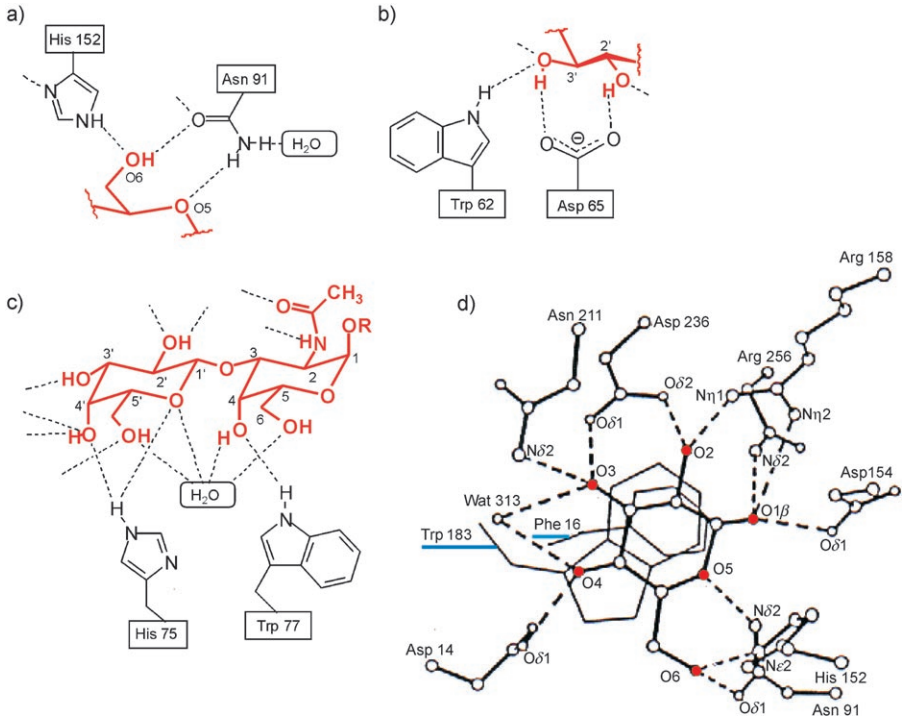

Figure 1. Examples of hydrogen bonds in the complex of a) galactose-binding protein with D-glucose,[1a] b) maltose-binding protein with maltose[1b] and c) *Amaranthus caudatus* with benzyl α-glycoside of Galβ3GalNAc.[1i] d) Intermolecular hydrogen bonds and stacking interactions in the complex between D-glucose and galactose-binding protein (adapted from reference [1a]; the glucose is sandwiched between the indole of Trp183 and the phenyl ring of Phe16).

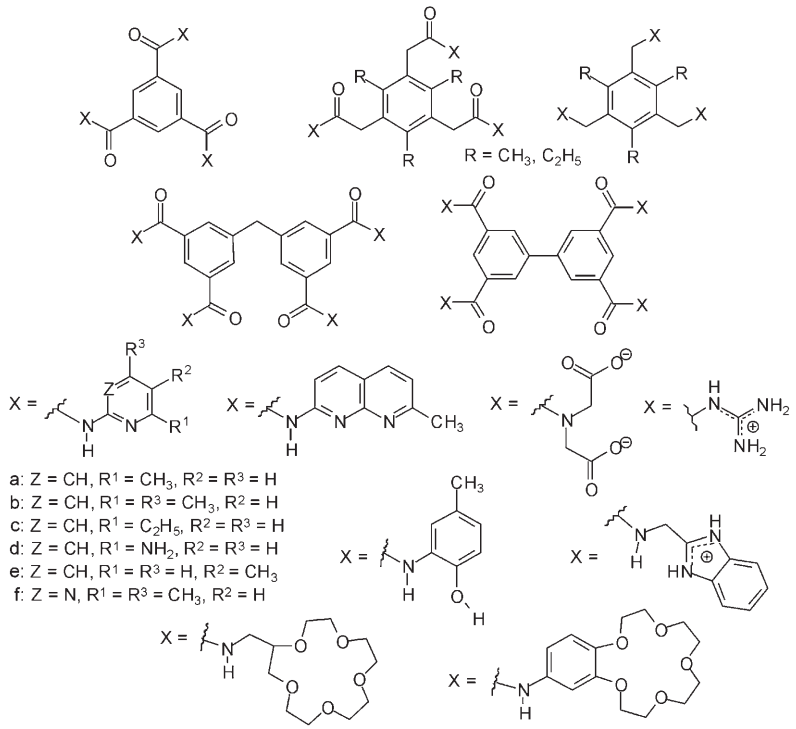

Scheme 1. Examples of spacer and recognition units X that were used by our group for the construction of acyclic carbohydrate receptors.[3b–d,g–j,s,t,4k,s,t]

see Scheme 2). The design of these receptors was inspired by the binding motifs shown in Figure 1; the imidazole or indole group is able to participate in both hydrogen bonding (Figure 1a, b and c) and stacking interactions with the sugar ring (Figure 1d). Figure 1a shows the participation of both the imidazole ring and the amide group of galactose-binding protein in hydrogen bonding with D-glucose. To mimic such a combination of noncovalent interactions, the 2-aminopyridine unit was incorporated into the receptor structure as a heterocyclic analogue of the asparagine/glutamine primary amide side chain (see also reference [6]). Our previous binding studies showed that aminopyridines provide an excellent structural motif for binding carbohydrates. This is associated with the ability to form cooperative and bidentate hydrogen bonds with the sugar OH groups.[3g,s,t,4k,s,t] As in previously described artificial systems (Figure 2),[3j] the participation of the phenyl ring of the receptor in the interactions with sugar C–H units was expected to provide additional stabilisation of the receptor–sugar complexes (the character of carbohydrate–aromatic interactions is still a subject of controversy; see reference [7]). In addition, we describe comparative binding studies with compounds **3** and **4**, which incorporate a 2-substituted pyrrole or 1-substituted imidazole group, respectively (see Scheme 2).

Quiochio has shown that the hydrogen bonds between sugar-binding proteins and essential recognition determinants on sugars are shielded from the bulk solvent, meaning that they exist in an environment with a lower dielectric constant[1a] (see also reference [8]). Thus, investigations

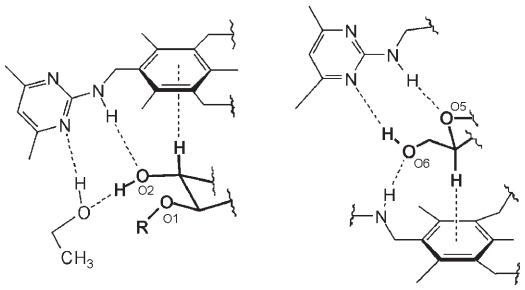

Figure 2. Examples of binding motifs observed in the crystal structure of the 2:1 receptor–sugar complex formed between pyrimidine-based receptor[3j] and octyl β-D-glucopyranoside.

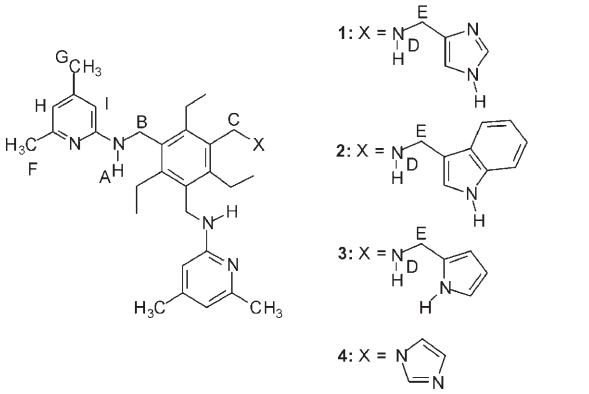

Scheme 2. Structures of receptors **1**–**4**.

with synthetic receptors in organic media make an important contribution to our understanding of the complex carbohydrate binding processes in nature (recognition of neutral sugars in aqueous solution through noncovalent interactions remains an important challenge in artificial receptor chemistry; for some examples, see references [3h,l,9]).

To evaluate the recognition capabilities of receptors **1**–**4** in organic media and compare their binding properties with the properties of the previously published receptors, the octyl β-D-glucopyranoside (**5**), octyl α-D-glucopyranoside (**6**), octyl β-D-galactopyranoside (**7**), dodecyl β-D-maltoside (**8**) and dodecyl α-D-maltoside (**9**) were selected as substrates.

The interactions of the receptors and carbohydrates were

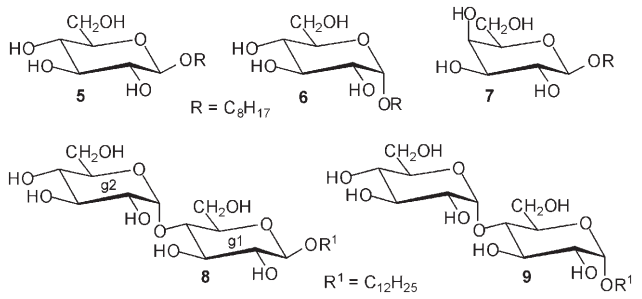

investigated by ^{1}H NMR and fluorescence spectroscopy. The ^{1}H NMR binding titration data were analysed by using the Hostest 5.6[10] and the HypNMR programs[11a] (stoichiometry of the receptor–sugar complexes was determined by mole ratio plots and by the curve-fitting analysis of the titration data). The fluorescence binding titration data were analysed by using the Hyperquad program.[11b]

Results and Discussion

Synthesis of the receptors: The synthesis of compounds **1**–**4** started from 1,3,5-tris(bromomethyl)-2,4,6-triethyl benzene (**10**),[12] which was converted into compound **11** through a reaction with two equivalents of 2-amino-4,6-dimethylpyridine. The separation of the product **11** and the byproducts **11a** and **11b** (see Scheme 3) was carried out by column chromatography. The crystal structure of **11** is shown in Figure 3; it should be noted that the three arms of **11** point to the same face of the central phenyl ring, whereas the three ethyl groups point in the opposite direction. The reaction of **11** with aqueous ammonia gave the amino derivative **12**, which was the base for the synthesis of compounds **1**–**3**. The reaction of **12** with one equivalent of the corresponding carbaldehyde, such as 4(5)-imidazole-carbaldehyde (for a discussion on annular NH tautomerism of imidazoles, see reference [13]), 3-indole-carbaldehyde or 2-pyrrole-carbaldehyde, provided the corresponding imine (for example, compound **13**, as shown in Scheme 3), which was further reduced with sodium borohydride. Compound **4** was synthesised by reaction of **11** with one equivalent of imidazole (see the Experimental Section).

Binding properties of receptors 1 and 2 toward β-glucopyranoside 5: The ^{1}H NMR titration experiments[14] with β-glucopyranoside **5** were carried out by adding increasing amounts of the sugar to a $CDCl_3$ solution of the receptor **1** or **2**. In addition, inverse titrations were performed in which the concentration of sugar **5** was held constant and that of the receptor was varied.

The complexation between the receptors **1** or **2** and β-glucopyranoside **5** was evidenced by several changes in the NMR spectra (see Figures 4, 5, and 6). After the addition of one equivalent of sugar **5** to a solution of the receptor **1** or **2**, almost no more change was observed in the chemical shift of the receptor signals.

During the titration of **1** with **5**, the signal due to the amine NH^A of **1** (for labelling, see Scheme 2) moved downfield by about 1.5 ppm with broadening (see Figure 4d); the NH^D signal showed very strong broadening and was unobservable after the addition of only 0.1 equivalents of **5**. Furthermore, the ^{1}H NMR spectra showed changes in the chemical shifts of the CH_3 (protons F, G), CH_2 (protons B, C, E), pyridine CH (protons H, I) and imidazole CH resonances of **1** (see Figure 4a, b, c and e). The signal for the protons B moved upfield by 0.17 ppm with broadening, whereas those for the protons C and E shifted down- and upfield by 0.05 ppm (splitting of the CH_2^C signal of **1** was observed after the addition of about 0.3 equivalents of **5**; see Figure 4b). The two imidazole CH protons shifted downfield by

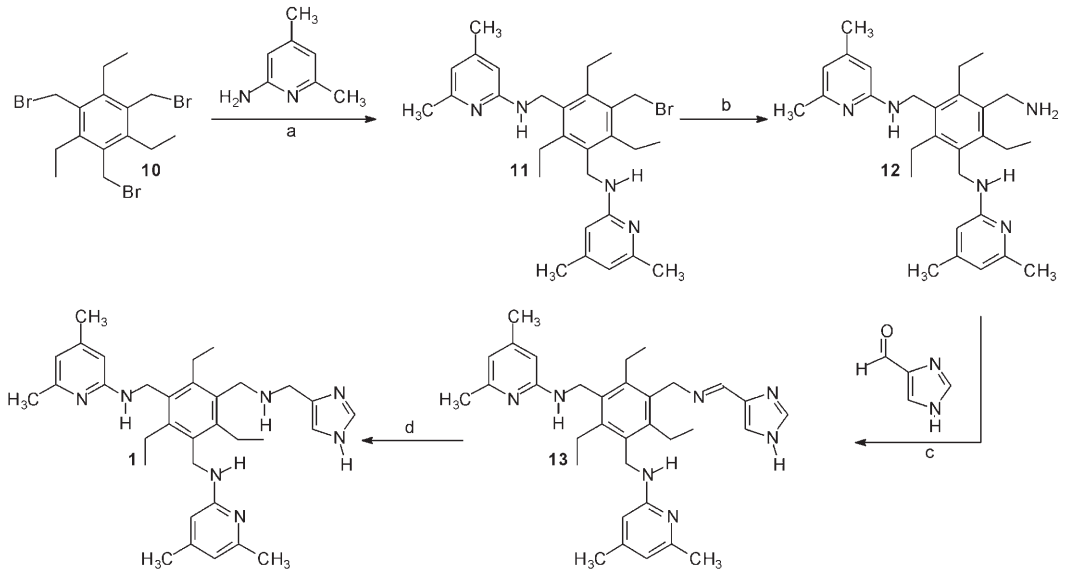

Scheme 3. Reaction conditions: a) 2-amino-4,6-dimethylpyridine (2 equiv), CH_3CN/THF, K_2CO_3, 48 h (30%); byproducts **11a** and **11b**: 1,3-bis(bromomethyl)-5-[(4,6-dimethylpyridin-2-yl)aminomethyl]-2,4,6-triethylbenzene and 1,3,5-tris[(4,6-dimethyl-pyridin-2-yl)aminomethyl]-2,4,6-triethylbenzene; b) NH_3/H_2O (25% solution), 12 h (72%); c) 4(5)-imidazole-carbaldehyde (1 equiv), CH_3OH, 24 h; d) $NaBH_4$ (1.2 equiv, 32%).

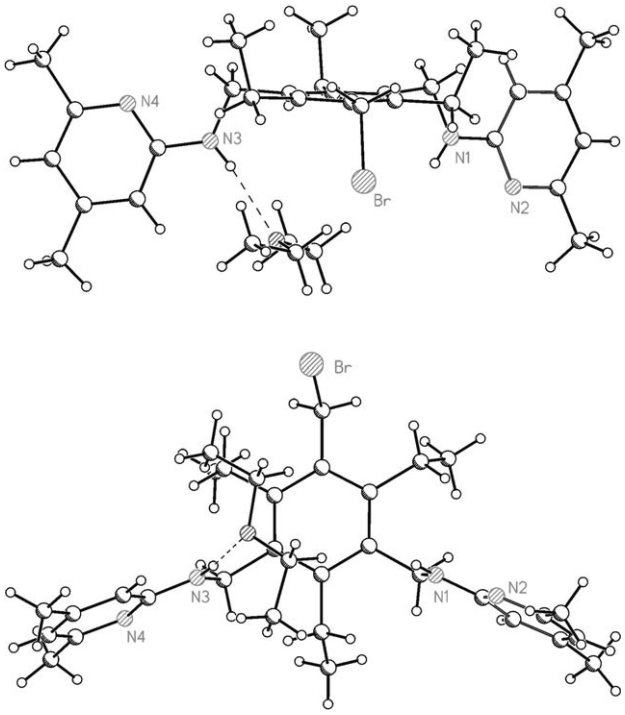

Figure 3. Crystal structure of **11**, side (upper image) and top (lower image) views (the hydrogen-bonded diethyl ether molecule is shown).

0.03 and 0.08 ppm (see Figure 4f). The NH^A, CH_2^B, CH_3^F and imidazole CH signals were monitored for the determination of the binding constants; the typical titration curves are shown in Figure 5a and b. The best fit of the titration data was obtained with the mixed 1:1 and 2:1 receptor–sugar binding model; this model was further supported by mole-ratio plots (see Figure S5 in the Supporting Information). The binding constants for **1·5** were found to be 191730 M^{-1} (K_{11}) and 8560 M^{-1} (K_{21}; $\beta_{21}=1.64\times10^9\,M^{-2}$; Table 1).[14c]

The addition of β-glucopyranoside **5** to a solution of the receptor **2** also caused significant downfield shift of the amine NH^A signal of **2** as well as changes in the chemical shifts of the indole NH, $CH_3^{F,G}$, $CH_2^{B,C,E}$ (see Figure 6), indole CH and pyridine $CH^{H,I}$ resonances. The signal for the protons A moved by about 1.9 ppm with broadening, whereas those for the protons F, G, H and I shifted in the range 0.03–0.08 ppm. The CH_2^B (see Figure 6b) and CH_2^E signals moved upfield by 0.20 and 0.03 ppm, respectively, whereas the CH_2^C signal shifted downfield by 0.08 ppm (see Figure 6b). The signals for the protons C and E were overlapping during the titration, the indole NH signal shifted downfield with very strong broadening and the NH^D signal of **2** was unobservable after the addition of only 0.1 equivalent of **5**; these signals could not be used for the determination of the binding constants. Both the curve fitting of the titration data (the complexation-induced chemical shifts of the NH^A, CH_2^B and $CH_3^{F,G}$ signals were analysed) and the mole-ratio plots suggested again the existence of 1:1 and 2:1 receptor–sugar complexes in the chloroform solution, with the stronger association constant for 1:1 binding and a weaker association constant for the 2:1 receptor–sugar complex. The association constants for **2·5** were determined to be 156100 M^{-1} (K_{11}) and 10360 M^{-1} (K_{21}; $\beta_{21}=1.62\times10^9\,M^{-2}$; Table 1).

The high values of the binding constants for **1·5** and **2·5** determined on the base of the ^1H NMR spectroscopic titrations were confirmed by a second, independent technique, namely fluorescence spectroscopy[15] (for a discussion on limitations of the NMR method, see reference [16]). The analysis of the fluorescence titration data (fluorescence intensity

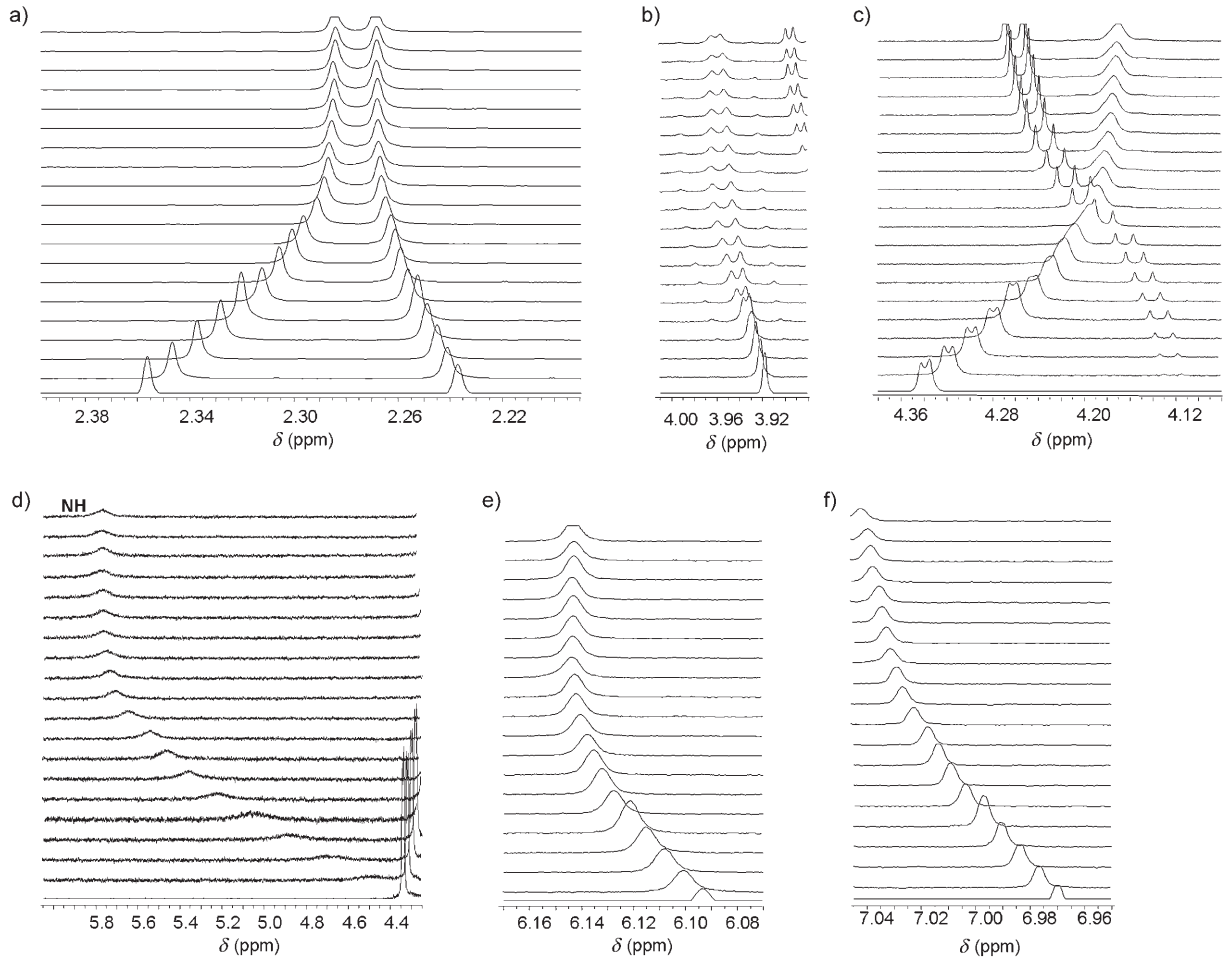

Figure 4. Partial ^{1}H NMR spectra (500 MHz; $CDCl_3$) of receptor **1** after the addition of (from bottom to top) 0.00, 0.10, 0.21, 0.32, 0.43, 0.54, 0.65, 0.76, 0.87, 1.09, 1.31, 1.53, 1.75, 1.97, 2.19, 2.41, 2.63, 2.85, 3.07 and 3.28 equivalents of **5** ([1] = 0.98 mM). Shown are chemical shifts of the a) CH_3^F and CH_3^G, b) CH_2^C, c) CH_2^B, d) NH^A, e) pyridine CH^I and f) imidazole CH resonances of **1** (for labelling, see Scheme 2).

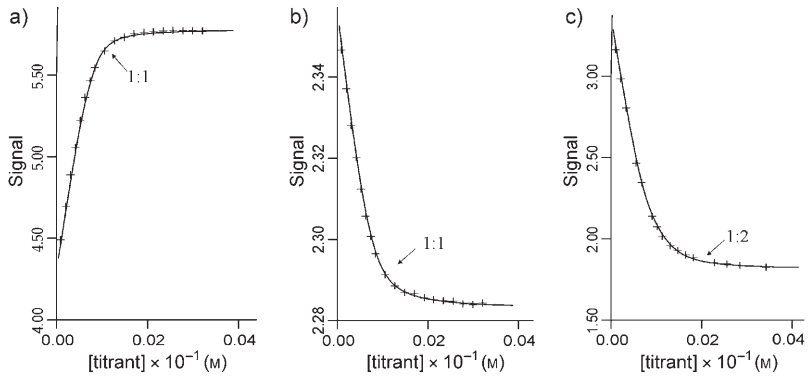

Figure 5. a and b) Plot of the chemical shifts of the NH^A (downfield shift) and CH_3^F (upfield shift) of **1** as a function of added β-glucopyranoside **5**. The [receptor]:[sugar] ratio is marked. c) Chemical shift changes observed for the 2-CH group of **5** during the titration of **5** with **1** (inverse titration). The [sugar]:[receptor] ratio is marked.

decreased with increasing monosaccharide concentration) confirmed also the mixed 1:1 and 2:1 receptor–glucopyranoside binding model; the binding constants determined on the base of fluorescence titrations in $CHCl_3$ were comparable with those determined on the base of the NMR spectroscopic titrations.

In addition, the interactions between β-glucopyranoside **5** and the receptors **1** and **2** were investigated on the base of inverse titrations in which the concentration of sugar **5** was held constant and that of receptor **1** or **2** varied. During the titration of **5** with **1** or **2**, the signals due to the OH protons of **5** shifted downfield with strong broadening and were unobservable after the addition of only 0.1 equivalent of the receptor (see Figure 7b), indicating the important contribution of the OH groups of **5** to the complex formation. The complexation between **5** and the receptor **1** or **2** was further evidenced by significant chemical-shift changes of the CH units of **5** (for examples,

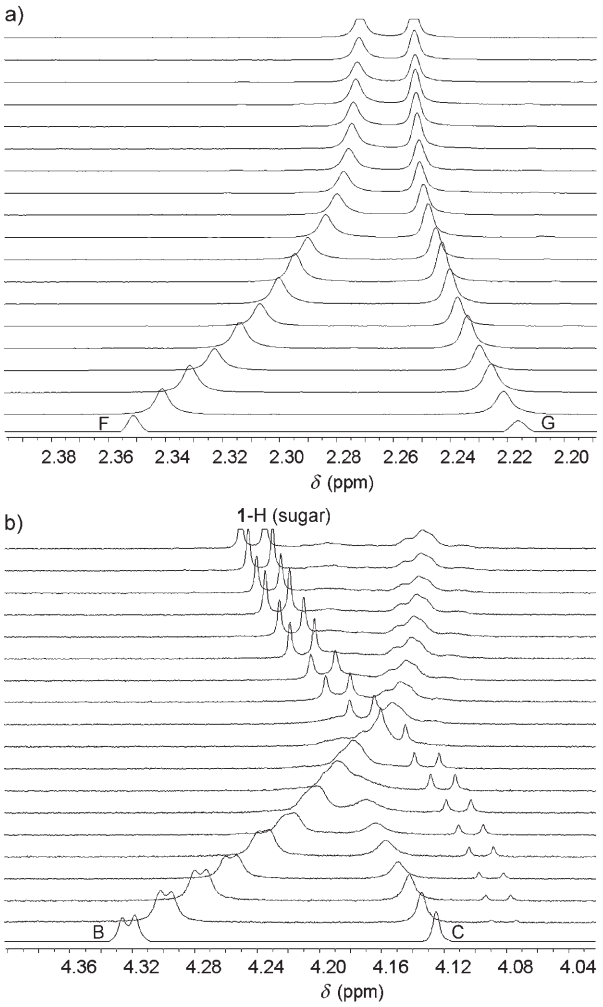

Figure 6. Partial ^{1}H NMR spectra (500 MHz; $CDCl_3$) of receptor **2** after the addition of (from bottom to top) 0.00, 0.11, 0.22, 0.32, 0.43, 0.54, 0.65, 0.76, 0.87, 1.09, 1.30, 1.52, 1.74, 1.96, 2.18, 2.39, 2.61, 2.83, 3.05 and 3.27 equivalents of **5** ([2] = 0.99 mM). Shown are the chemical shifts of the a) $CH_3^{F,G}$ and b) $CH_2^{B,C}$ resonances of **2** (for labelling, see Scheme 2).

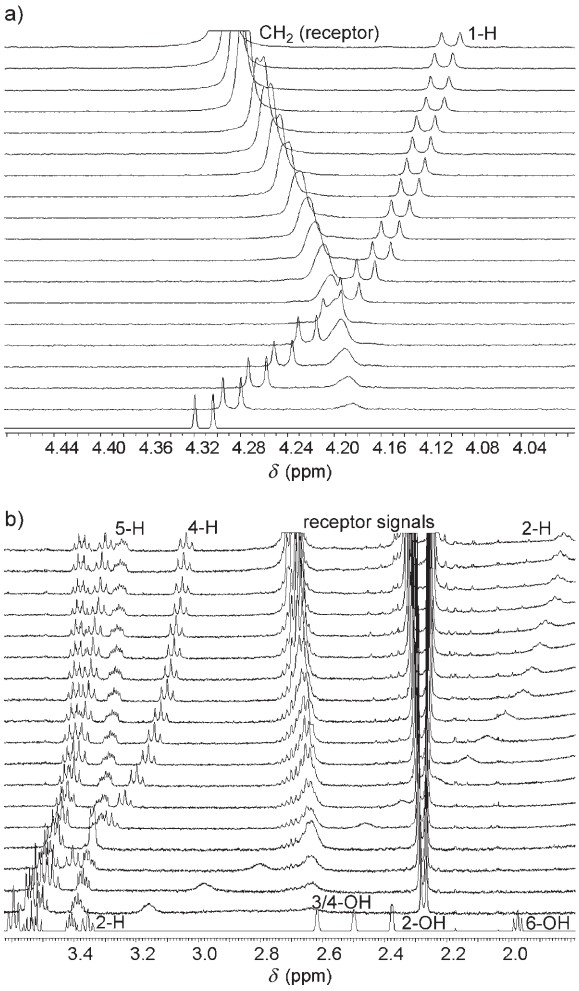

Figure 7. Partial ^{1}H NMR spectra (500 MHz; $CDCl_3$) of β-glucopyranoside **5** after the addition of (from bottom to top) 0.00, 0.15, 0.32, 0.49, 0.65, 0.81, 0.98, 1.14, 1.30, 1.47, 1.63, 1.87, 2.12, 2.36, 2.61, 3.26, 3.67, 4.08 and 4.89 equivalents of **1** ([5] = 0.70 mM). Shown are the chemical shifts of the a) CH-1 and b) CH-2,-3,-4, and CH-5 resonances of **5**.

see Figure 7a and b). During the titrations of **5** with **1**, the signals due to the 1-, 2-, 3-, 4- and 5-CH protons of **5** shifted upfield by 0.21, 1.53, 0.29, 0.55 and 0.18 ppm, respectively (after the addition of about 4 equivalents of receptor **1**). The titrations of **5** with **2** caused upfield shifts of the 1-, 2-, 4- and 5-CH signals of **5** by 0.25, 1.72, 0.61 and 0.15 ppm, respectively. These complexation-induced chemical-shift changes are significantly larger than those usually reported for the CH protons of β-glucopyranoside in the literature. Among the CH signals, the signals due to the 2-CH and 4-CH protons of **5** show the largest shift, suggesting a particularly important contribution of these CH units to the complex stabilisation (through formation of CH···π interactions with the phenyl ring of the receptor). The participation of the CH units of **5** in CH···π interactions with the central phenyl ring of the receptor was also indicated by molecular modelling (see below, Table 2, Figure 8). In both cases, **5·1** and **5·2**, the best fit of the titration data was obtained with the mixed 1:1 and 1:2 sugar–receptor binding model (for example, see Figure 5c); thus, the inverse titrations supported the existence of 1:1 and 2:1 receptor–sugar complexes in chloroform solution, with a stronger association constant for 1:1 binding and a weaker association constant for the 2:1 receptor–sugar complex. The association constants obtained on the base of these titrations are identical within the limits of uncertainty to those determined from titrations in which the role of the receptor and substrate was reversed.

Molecular-modelling studies suggested that all OH groups and the ring oxygen atom of the bound sugar **5** in the complex **1·5** are involved in the formation of hydrogen bonds (see Table 2). Interactions of sugar C–H bonds with the central phenyl ring of **1** (2-CH···π and 4-CH···π interactions; see Figure 8a) provide additional stabilisation of the complex. Furthermore, the molecular-modelling calculations indicated that in the 2:1 receptor–sugar complex, the two receptor molecules almost completely enclose the sugar, leading to

Table 1. Association constants[a,b] for receptors **1**–**4** and carbohydrates **5**–**9**.

Host–guest complex	K_{11} [M^{-1}]	K_{21}[c] or K_{12}[d] [M^{-1}]	$\beta_{21}=K_{11}K_{21}$ or $\beta_{12}=K_{11}K_{12}$ [M^{-2}]	$\Delta\delta_{obs}$[e] [ppm]
1·5	191730	8560[c]	1.64×10^9	NH: 1.50; CH_2: −0.17; CH_3: −0.08 1-CH: −0.21; 2-CH: −1.53; 4-CH: −0.55
1·6	3160	1540[d]	4.86×10^6	NH: 1.11; CH_2: −0.14; CH_3: −0.06 1-CH: −0.22; 2-CH: −0.67 ; 4-CH: −0.55
1·7	3320	300[d]	9.96×10^5	NH: 1.20; CH_2: −0.13; CH_3: −0.05
1·8	205760	8670[c]	1.78×10^9	NH: 1.34; CH_2: −0.13; CH_3: −0.06
1·9	147200	6450[c]	9.49×10^8	NH: 1.39; CH_2: −0.17; CH_3: −0.06
2·5	156100	10360[c]	1.62×10^9	NH: 1.85; CH_2: −0.20; CH_3: −0.08 1-CH: −0.25; 2-CH: −1.72; 4-CH: −0.61
2·6	2820	350[d]	9.87×10^5	NH: 1.17; CH_2: −0.14; CH_3: −0.05
2·7	7470	1100[d]	8.25×10^6	NH: 1.21; CH_3: −0.05
2·8	182690	14840[c]	2.71×10^9	NH: 1.32; CH_2: −0.17; CH_3: −0.06
2·9	123650	10390[c,f]	1.28×10^9	
3·5	179370	7470[c]	1.34×10^9	NH: 1.60, CH_2: −0.18; CH_3: −0.08 1-CH: −0.21; 2-CH: −1.60; 4-CH: −0.56
3·6	2300	–	–	NH: 1.17; CH_2: −0.15, CH_3: −0.06
3·7	4100	–	–	NH: 1.22; CH_2: −0.13, CH_3: −0.06
4·5	3560	1300[d]	4.87×10^6	NH: 0.98; CH_2: −0.08; CH_3: −0.03
11b·5[g]	48630	1320[d]	6.42×10^7	NH: 1.31; CH_2: −0.16; CH_3: −0.07

[a] Average K_a values from multiple titrations in $CDCl_3$ (the high values of the binding constants for **1·5**, **2·5**, **1·8** and **2·8** determined on the basis of the ^1H NMR spectroscopic titrations were confirmed by fluorescence titrations). [b] Errors in K_a are less than 10%. [c] K_{21} corresponds to 2:1 receptor–sugar association constant. [d] K_{12} corresponds to 1:2 receptor–sugar association constant. [e] Largest change in chemical shift observed during the titration for NH^A, $CH_2{}^B$ and $CH_3{}^F$ signals of the receptor (the concentration of receptor was kept constant and that of sugar varied) as well as for the 1-CH, 2-CH or 4-CH groups of the sugar in the case of inverse titrations (the concentration of sugar was kept constant and that of the receptor was varied). [f] Determined only on the basis of fluorescence titrations. [g] Results from reference [3s], compound **11b**: 1,3,5-tris[(4,6-dimethylpyridin-2-yl)aminomethyl]-2,4,6-triethylbenzene.

Table 2. Examples of noncovalent interactions indicated by molecular-modelling calculations[a] for the complexes formed between receptor **1** and sugars **5** and **8**.

Receptor–substrate system	1:1 Receptor–sugar complex[b]	2:1 Receptor–sugar complex[c]
1·5	pyridine-N···HO-2	(I) imidazole-NH···OH-2
	NH^A···OH-2	(II) imidazole-NH···OH-2; (II) HN^D···HO-2
	NH^D···OH-3	(I) pyridine-N···HO-3; (II) NH^A···OH-3
	imidazole-NH···OH-3	(II) pyridine-N···HO-4; (I) NH^A···OH-4
	imidazole-HN···HO-4	(II) pyridine-N···HO-6
	HN^D···HO-4	(II) NH^A···O-ring; (II) NH^D···O-1
	pyridine-N···HO-6	(I) phenyl···HC-1; (I) phenyl···HC-3
	NH^A···O-ring	(I) phenyl···HC-5; (II) phenyl···HC-2
	phenyl···HC-2; phenyl···HC-4	(II) phenyl···HC-4
1·8	pyridine-N···HO-2 (g1)	(I) imidazole-NH···OH-2 (g1)
	NH^A···OH-2 (g1)	(I) HN^D···HO-2 (g1)
	NH^D···OH-3 (g1)	(I) NH^D···OH-3 (g1)
	imidazole-NH···OH-3 (g1)	(I) NH^A···O-1 (g1)
	pyridine-N···HO-6 (g1)	(II) NH^A···OH-2 (g2)
	NH^A···O-ring (g1)	(I) pyridine-N···HO-2 (g2)
	imidazole-HN···HO-2 (g2)	(II) NH^A···OH-3 (g2)
	phenyl···HC-2 (g1)	(II) pyridine-N···HO-4 (g2)
	phenyl···HC-4 (g1)	(II) NH^D···O-ring (g2)
	imidazole···HC-3 (g2)	(I) phenyl···HC-1 (g1); (I) phenyl···HC-3 (g1)
		(I) phenyl···HC-5 (g1); (II) imidazole···HC-2 (g1)
		(II) imidazole···HC-4 (g1); (II) phenyl···HC-2 (g2)

[a] MacroModel V.8.5, OPLS-AA force field, MCMM, 50000 steps. [b] g1 and g2: the glucose units of **8**. [c] I and II: the two receptors molecules in the 2:1 receptor–sugar complex.

involvement of all sugar hydroxy groups in interactions with the two receptor molecules (see Table 2, Figure 8b). The OH groups are involved in the formation of cooperative hydrogen bonds resulting from the simultaneous participation of a sugar OH as the donor and acceptor of hydrogen bonds. The phenyl units of both receptors stack on the sugar ring; both sides of the pyranose ring are involved in CH···π interactions (see Table 2 and Figure 8b).

The comparison of the binding properties of the receptors **1** and **2** with those of the previously described three-armed pyridine-based analogues[3s,4k] shows that the incorporation of a suitable substituted imidazole or indole unit into the acyclic receptor structure significantly affects the binding affinity and selectivity of the new receptors (for comparison of the binding constants, see Table 1). As in natural complexes, the high binding affinity and selectivity of the receptors **1** and **2** is achieved through the participation of different types of binding units in the recognition process.

Binding properties of receptors 1 and 2 toward monosaccharides 6 and 7: Binding studies with α-glucopyranoside **6** and β-galactopyranoside **7** showed that the interactions of receptors **1** and **2** with these monosaccharides are less favourable than those with β-glucopyranoside **5**. Similar to the binding studies with sugar **5**, the complexation between receptors **1** and **2** and pyranosides **6** and **7** was evidenced by several changes in the NMR spectra. With the monosaccharides **6** and **7**, chemical shift changes continue to higher [sugar]/[receptor] ratios, indicating lower affinity of **1** and **2** toward **6** and **7**, whereas after the addition of

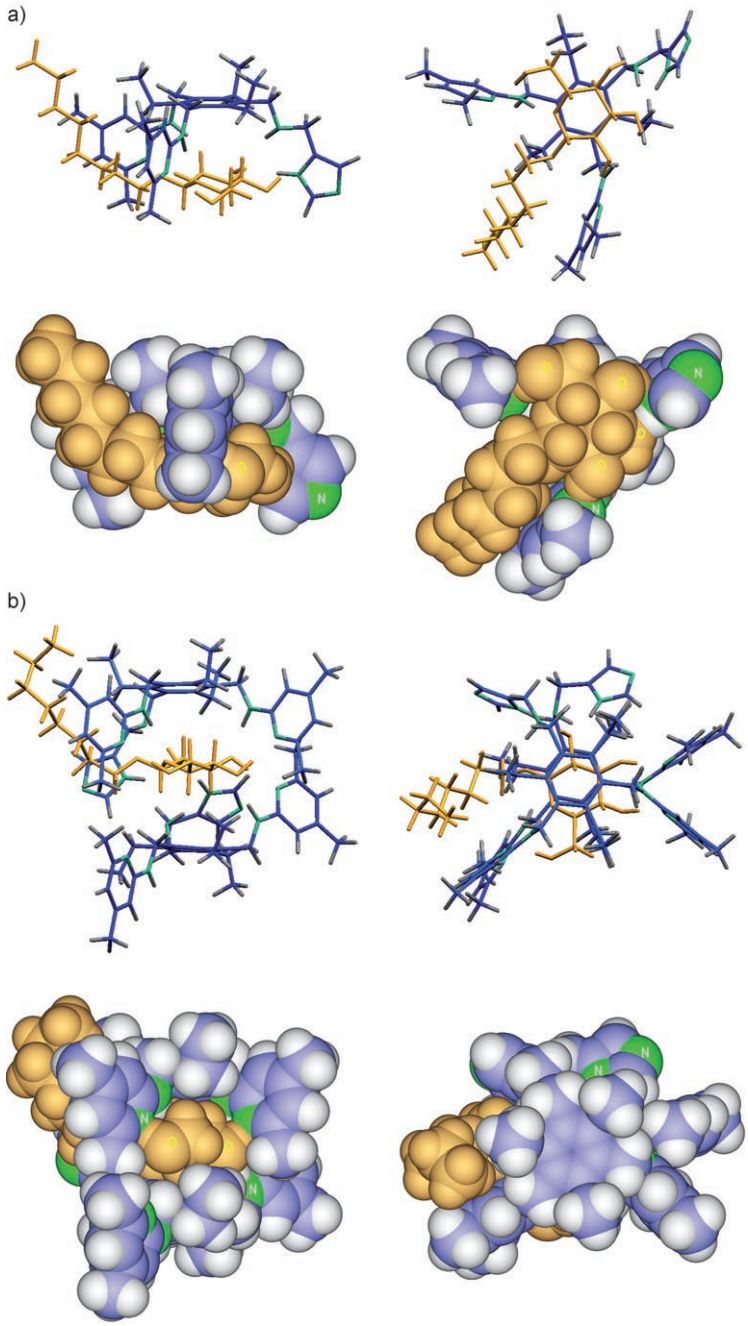

Figure 8. Energy-minimised structure of a) the 1:1 complex formed between receptor **1** and β-glucopyranoside **5** (different representations) and b) the 2:1 complex between receptor **1** and β-glucopyranoside **5** (different representations). MacroModel V.8.5, OPLS-AA force field, MCMM, 50000 steps. Colour code: receptor C, blue; receptor N, green; sugar molecule, yellow.

one equivalent of β-glucopyranoside **5**, almost no further change was observed in the chemical shift of the receptor signals. During the titration of **1** and **2** with α-glucopyranoside **6**, the signal due to the amine NH^{A} of the receptor moved downfield by about 1.1 and 1.2 ppm, respectively (after the addition of about four equivalents of **6**). Furthermore, the ^{1}H NMR titrations of **1** or **2** with **6** produced chemical shift changes of the $CH_2^{B,C,E}$, $CH_3^{F,G}$, pyridine $CH^{H,I}$ as well as imidazole CH groups (in the range of 0.02–0.14 ppm). In contrast with the titrations with β-glucopyranoside **5**, no splitting of the CH_2^{C} signal of **1** was observed after the addition of the α-anomer **6**. The curve fitting of the titration data indicated the formation of complexes with 1:1 and 1:2 receptor–sugar stoichiometry (different binding model than that determined for the receptor **1** and **2** and β-glucopyranoside **5** (see Figure S1a in the Supporting Information); the binding constants for **1·6** were found to be $3160\,M^{-1}$ (K_{11}) and $1540\,M^{-1}$ (K_{12}; $\beta_{12}=4.86\times10^{6}\,M^{-2}$) and those for **2·6** were $2820\,M^{-1}$ (K_{11}) and $350\,M^{-1}$ (K_{12}; $\beta_{12}=9.87\times10^{5}\,M^{-2}$; see Table 1).

The interactions between α-glucopyranoside **6** and the receptor **1** were also investigated on the base of inverse titrations (see Figure 9). The signals due to the OH protons of **6** shifted downfield with strong broadening and were unobservable after the addition of only 0.1 equivalents of the receptor **1** (similar to the titrations of **5** with **1**), indicating again the important contribution of the OH groups of **6** to the complex formation. The signals of the 1-, 2-, 3-, 4-, and 5-CH protons shifted upfield by 0.22, 0.67, 0.25, 0.55 and 0.15 ppm, respectively (after the addition of about 6 equivalents of receptor **1**). Similar to the titration of **5** with **1**, the signals due to the 2- and 4-CH group of the α-glucopyranoside **6** showed the largest shifts (however, the chemical-shift changes of the 2-CH signal of **6** are less substantial than those of the 2-CH signal of **5**). The analysis of the titration data indicated the formation of complexes with 1:1 and 2:1 sugar–receptor binding stoichiometry; thus, the inverse titrations fully confirmed the binding model determined through the titrations of the receptor **1** with the α-anomer **6** (see above). The association constants obtained on the basis of these titrations are again identical within the limits of uncer-

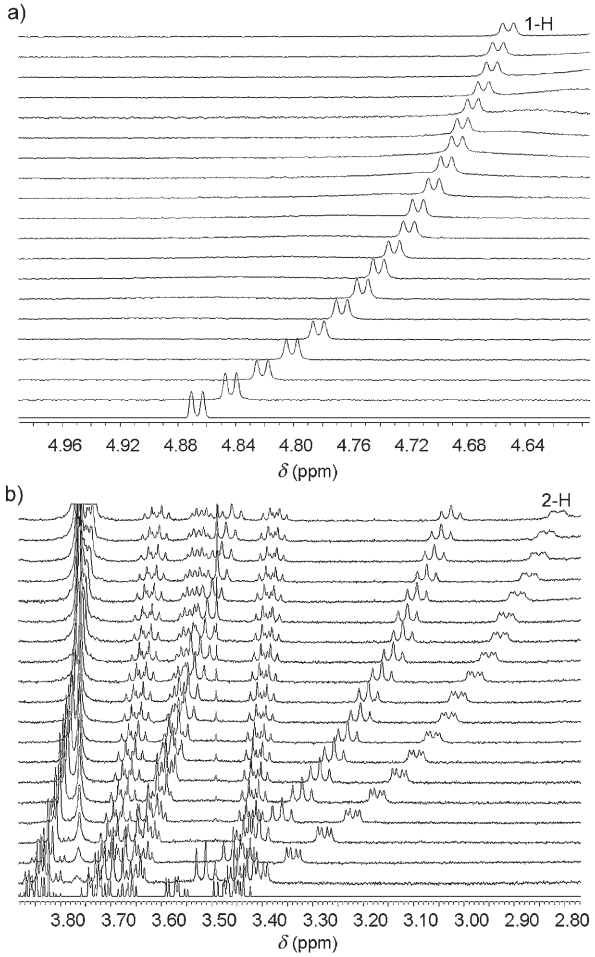

Figure 9. Partial ^{1}H NMR spectra (500 MHz; $CDCl_3$) of α-glucopyranoside **6** after the addition of (from bottom to top) 0.00, 0.20, 0.41, 0.62, 0.83, 1.04, 1.25, 1.46, 1.67, 1.88, 2.09, 2.40, 2.72, 3.03, 3.35, 3.66, 4.18, 4.71, 5.23 and 6.28 equivalents of **1** ([6] = 0.58 mM).

tainty to those determined from titrations in which the role of the receptor and substrate was reversed.

The ^{1}H NMR spectra obtained through titrations of receptor **1** and **2** with β-galactopyranoside **7** showed downfield shifting of the NH^A resonances of **1** and **2** by about 1.2 ppm (see Figure S1b in the Supporting Information). The signals for the $CH_3^{F,G}$ and pyridine $CH^{H,I}$ protons of **1** and **2** moved up- and downfield in the range of 0.02–0.06 ppm, whereas those for the CH_2^B protons shifted upfield by about 0.14 ppm. The analysis of the titration data with galactopyranoside **7** indicated the formation of complexes with 1:1 and 1:2 receptor–sugar stoichiometry. The binding constants for **1·7** were found to be 3320 M^{-1} (K_{11}) and 300 M^{-1} (K_{12}; $\beta_{12} = 9.96\times10^5\ M^{-2}$), whereas those for **2·7** were 7470 M^{-1} (K_{11}) and 1100 M^{-1} (K_{12}; $\beta_{12} = 8.25\times10^6\ M^{-2}$). Thus, the complexes formed between the receptors **1** and **2** and sugars **6** and **7** are much less stable than those formed with the β-glucopyranoside **5**.

Binding properties of receptors 1 and 2 towards disaccharides 8 and 9: β-Maltoside **8** is poorly soluble in $CDCl_3$, but could be solubilised in this solvent in the presence of the receptor **1** or **2**, indicating favourable interactions between the binding partners. Thus, the receptor in $CDCl_3$ was titrated with a solution of maltoside dissolved in the same receptor solution. During the titrations of **1** and **2** with **8**, the signal due to the amine NH^A moved downfield by about 1.3 ppm with broadening; the NH^D signal was unobservable after the addition of only 0.1 equivalents of **8**. The $CH_3^{F,G}$ signals shifted up- and downfield in the range of 0.03–0.06 ppm, as shown in Figure 10a. The saturation occurred after the addition of approximately 0.75 equivalents of **8**. The CH_2^B signal of **1** and **2** moved upfield by 0.13 and 0.17 ppm, respectively, whereas the pyridine CH resonances shifted in the range of 0.01–0.06 ppm. The imidazole CH resonances of **1** shifted downfield by 0.05 and 0.07 ppm with broadening. The indole NH signal showed broadening and downfield shifting by 0.31 ppm. Both the curve fitting of the titration data (typical titration curves are shown in Figure 10b and c) and the mole-ratio plots (see Figure S5 in the Supporting Information) suggested again the existence of 1:1 and 2:1 receptor–sugar complexes in the chloroform solution, with a stronger association constant for 1:1 binding and a weaker associa-

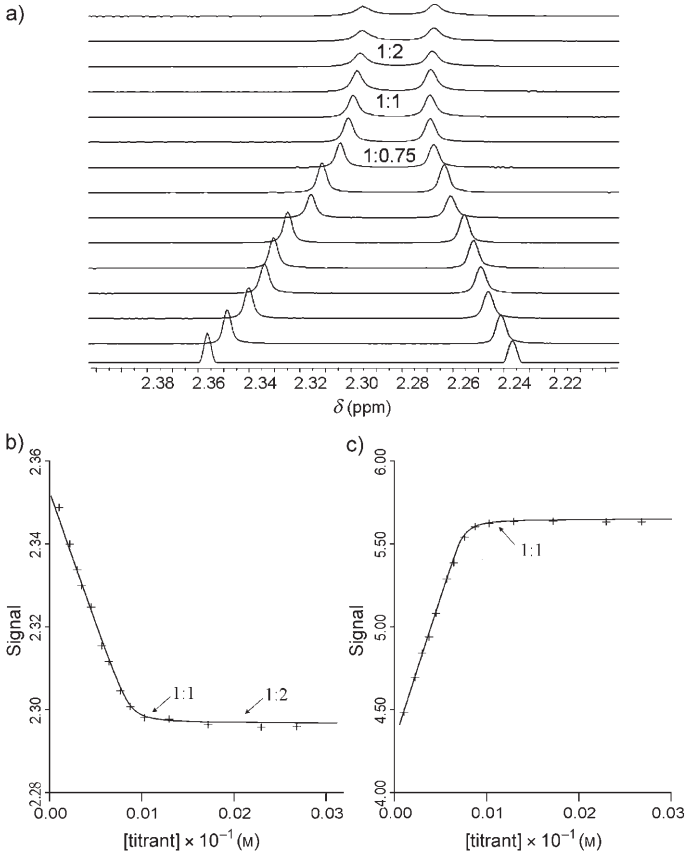

Figure 10. a) Partial ^{1}H NMR spectra (400 MHz, $CDCl_3$) of **1** after the addition of (from bottom to top) 0.00–2.73 equivalents of β-maltoside **8** ([1] = 0.98 mM). Shown are the chemical shifts of the $CH_3^{F,G}$ resonances of **1** (for labelling, see Scheme 2). b and c) Plot of the observed (+) and calculated (——) chemical shifts of the CH_3^F and NH^A resonances of **1** as a function of added β-maltoside **8**; the [receptor]:[sugar] ratio is marked.

tion constant for the 2:1 receptor–sugar complex. The association constants for **1·8** were determined to be 205760 M^{-1} (K_{11}) and 8670 M^{-1} (K_{21}; $\beta_{21} = 1.78 \times 10^9 M^{-2}$), those for **2·8** were found to be 182690 M^{-1} (K_{11}) and 14840 M^{-1} (K_{21}; $\beta_{21} = 2.71 \times 10^9 M^{-2}$).[17]

According to molecular-modelling calculations, the 1:1 complex formed between the receptor **1** and β-maltoside **8** can potentially be stabilised by several hydrogen bonds between the OH groups of the sugar and the amine NH^A and NH^D, the pyridine-N and imidazole-NH of the receptor (see Table 2 and Figure 11a). Furthermore, interactions of sugar CH groups with the phenyl group of the receptor molecule should provide additional stabilisation of the receptor–sugar complex (for example, the interactions between the 2- and 4-CH groups of the g1 unit of **8** and the phenyl ring of **1**; see Table 2). The 2:1 receptor–maltoside complex (see Figure 11b) can be stabilised by at least ten hydrogen bonds as well as several CH···π interactions (see Table 2). As shown in Figure 11b, the central phenyl rings of the two receptors stack on the two glucose rings of **8**; the 2-, 3- and 5-CH groups of the g1 unit interact with the phenyl ring of one receptor molecule, whereas the 2-CH group of the g2 unit interacts with the central phenyl ring of the other receptor. In addition, interactions of the 2- and 4-CH groups of the g1 unit with the imidazole group of one receptor molecule should provide additional stabilisation of the 2:1 receptor–sugar complexes.

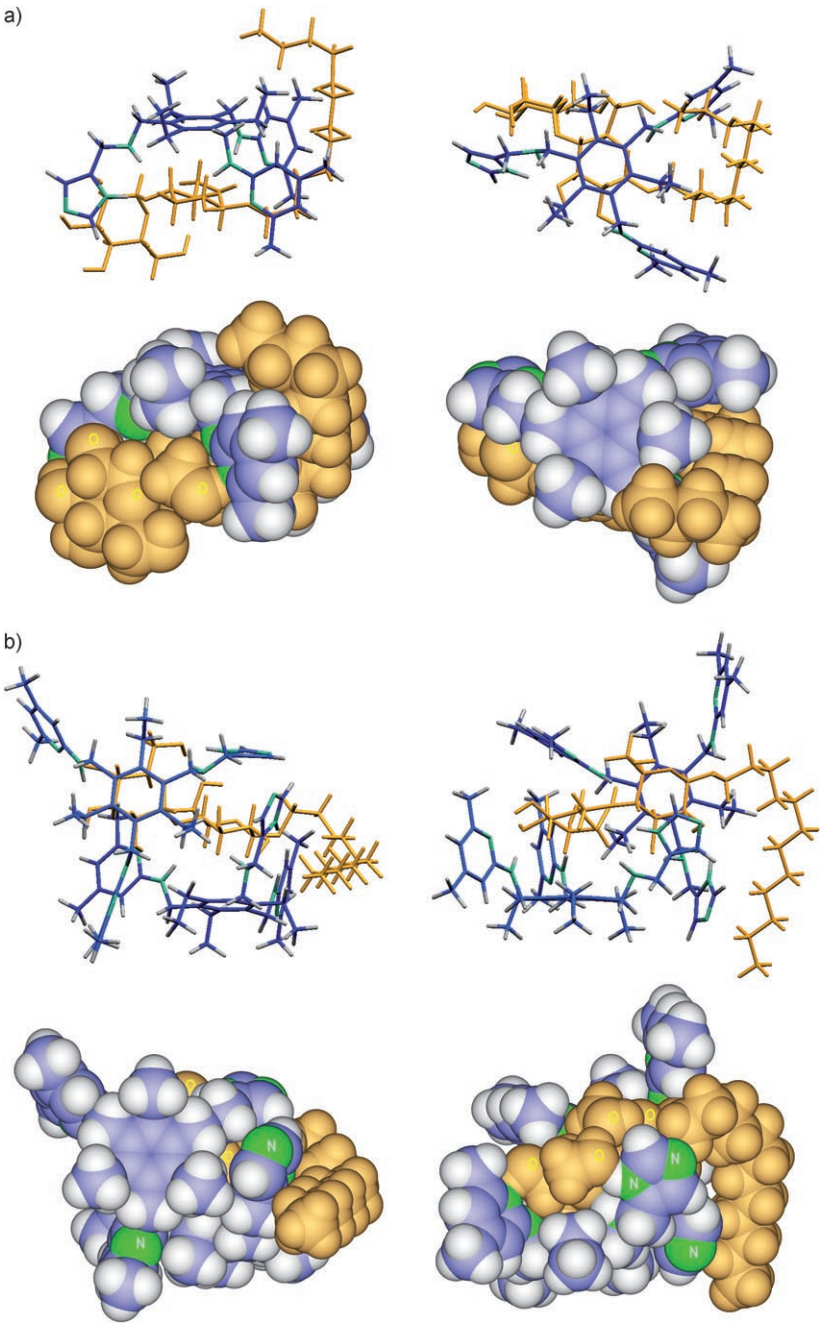

Figure 11. Energy-minimised structure of a) the 1:1 complex formed between receptor **1** and β-maltoside **8** (different representations) and b) the 2:1 receptor–sugar complex between receptor **1** and β-maltoside **8** (different representations). MacroModel V.8.5, OPLS-AA force field, MCMM, 50000 steps. Colour code: receptor C, blue; receptor N, green; sugar molecule, yellow.

α-Maltoside **9** is almost insoluble in $CDCl_3$ but could be solubilised in this solvent in the presence of the receptor **1**. The ^1H NMR titrations of **1** with α-maltoside **9** produced similar spectral changes as those with β-maltoside **8**. The fit of NMR shift changes of the NH^A and $CH_3{}^F$ resonances agreed again with the 1:1 and 2:1 receptor–sugar binding model; the binding constants for **1·9** were found to be 147200 M^{-1} (K_{11}) and 6450 M^{-1} (K_{21}; $\beta_{21} = 9.49 \times 10^8 M^{-2}$). Thus, ^1H NMR titrations indicated that the receptor **1** exhibits about a twofold higher affinity for β-maltoside **8** than for the α-anomer **9**.

The formation of strong complexes between the receptors **1** or **2** and disaccharides **8** and **9** was also confirmed by fluorescence spectroscopy. The fluorescence titration experiments were carried out by adding increasing amounts of the sugar **8** or **9** (both disaccharides are soluble in $CHCl_3$ in the

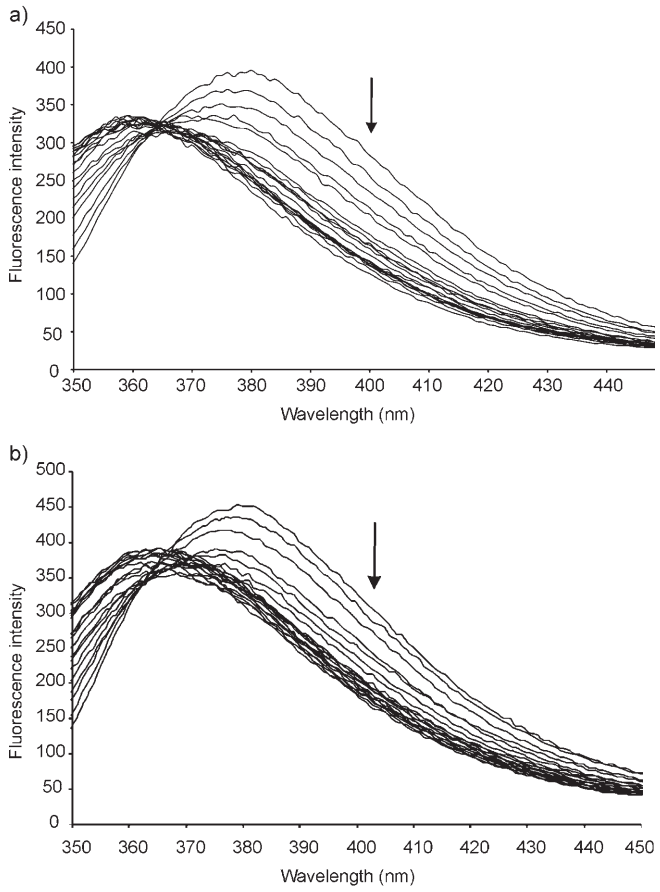

Figure 12. Fluorescence titration of receptor **2** with β-maltoside **8** (a) and α-maltoside **9** (b) in $CHCl_3$; [**2**] = 0.17 and 0.22 mM, respectively; equivalents of **8** = 0.00–3.40; equivalents of **9** = 0.00–3.37. Excitation wavelength 330 nm. The fluorescence intensity decreases with increasing concentration of **8** and **9** (see arrows).

concentration range required for fluorescence titrations) to a $CHCl_3$ solution of the receptor **1** or **2** (for example, see Figure 12). The best fit of the titration data was obtained with 1:1 and 2:1 receptor–sugar binding model; the formation of the 2:1 complexes was further supported by the mole-ratio plots. The binding constants for **1·8** were found to be 198580 M^{-1} (K_{11}) and 8900 M^{-1} (K_{21}; $\beta_{21} = 1.76 \times 10^9\ M^{-2}$), those for **2·8** amounted to 169900 M^{-1} (K_{II}) and 13810 M^{-1} (K_{21}; $\beta_{21} = 2.34 \times 10^9\ M^{-2}$). The K_{11} and K_{21} binding constants for **2·9** were found to be 123650 M^{-1} and 10390 M^{-1} ($\beta_{21} = 1.28 \times 10^9\ M^{-2}$), respectively. Thus, the binding constants are comparable with those determined on the basis of the NMR spectroscopic titrations.

Comparative binding studies with receptors 3 and 4: Molecular-modelling calculations indicated that the 3-N of the imidazole ring of **1** does not participate in the formation of hydrogen bonds with β-glucopyranoside **5**, as shown in Figure 8a. To evaluate the role of this nitrogen atom in the binding process, the pyrrole derivative **3** was synthesised and its binding properties toward **5** were studied. The binding studies showed that no significant difference in the binding efficiency was found between the receptors **3** and **1**, indicating a less important contribution of the imidazole 3-N of **1** to complex stabilisation. Thus, the results of the molecular-modelling calculations were confirmed by the experimental data.

The ^{1}H NMR titration experiments with β-glucopyranoside **5** were carried out by adding increasing amounts of the sugar to a $CDCl_3$ solution of the receptor **3** (Figure 13). Similar to the binding studies between **1** or **2** and **5**, the complexation between **3** and **5** was evidenced by several changes in the NMR spectra, as shown in Figure S2 in the Supporting Information. The signal due to the amine NH^A of **3** (for labelling, see Scheme 2) moved downfield by about 1.6 ppm with broadening (see Figure S2a in the Supporting Information), the CH_2^B and CH_2^E resonances moved upfield by 0.18 and 0.06 ppm, respectively, and the CH_2^C signal shifted downfield by 0.05 ppm (Figure S2b and c in the Supporting Information). The splitting of the CH_2^C signal of **3** was observed after the addition of about 0.2 equivalents of **5**, as shown in Figure S2c in the Supporting Information. Furthermore, the ^{1}H NMR spectra showed changes in the chemical shifts of the CH_3 group (protons F, G; see Figure S2d in the Supporting Information) and pyridine CH (protons H, I) resonances in the range of 0.03–0.08 ppm. The signal due to the pyrrole NH shifted downfield by 0.73 ppm with broadening. The curve fitting of the titration data suggested the existence of 1:1 and 2:1 receptor–sugar complexes in the chloroform solution; typical titration curves are shown in Figure 13a and Figure S2e in the Supporting Information. The binding constants for **3·5** were found to be 179370 M^{-1} (K_{11}) and 7470 M^{-1} (K_{21}; $\beta_{21} = 1.34 \times 10^9\ M^{-2}$); thus, the receptor **3**

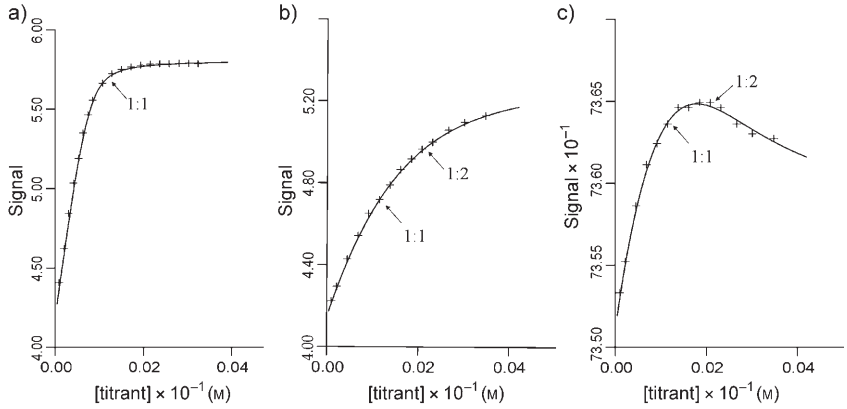

Figure 13. a) Plot of the chemical shifts of the NH^A resonances of **3** as a function of added **5**. Plot of the chemical shifts of the NH^A (b) and imidazole CH resonances (c) of **4** as a function of added **5** in $CDCl_3$. The [receptor]:[sugar] ratio is marked.

exhibits a similar level of affinity towards β-glucopyranoside as the receptors **1** and **2** (see Table 1).

The interactions between receptor **3** and β-glucopyranoside **5** were also investigated on the basis of inverse titrations in which the concentration of sugar **5** was held constant. Similar to the inverse titrations with receptors **1** and **2**, during the titration of **5** with **3**, the signals due to the OH protons of sugar **5** shifted downfield with strong broadening and were almost unobservable after the addition of only 0.1 equivalents of the receptor (see Figure S3b in the Supporting Information), indicating again the important contribution of the OH groups of **5** to complex formation. The complexation between **5** and the receptor **3** was further evidenced by significant chemical shift changes of the CH units of **5** (for examples see Figure S3a and b in the Supporting Information). The signals due to the 1-, 2-, 3-, 4- and 5-CH protons shifted upfield by 0.21, 1.60, 0.26, 0.56 and 0.17 ppm, respectively (after the addition of about 4 equivalents of receptor **3**), indicating the participation of the CH units of **5** in the formation of CH···π interactions with the aromatic ring of the receptor **3**.

In contrast with the strong binding of **3** with β-glucopyranoside **5**, the binding of α-glucopyranoside **6** and β-galactopyranoside **7** is relatively weak. The ^{1}H NMR titrations of **3** with **6** and **7** produced similar spectral changes as those with β-glucopyranoside **5**; however, saturation occurred after the addition of more than four equivalents of **6** or **7.** The ^{1}H NMR spectra showed changes in the chemical shifts of the NH^A (downfield shift by about 1.2 ppm), $CH_2^{B,C,E}$ (up- and downfield shifts in the range of 0.03–0.15 ppm), $CH^{H,I}$ and $CH_3^{F,G}$ (up- and downfield shifts in the range of 0.02–0.06 ppm) resonances of **3**. The best fit of the titration data was obtained with the 1:1 binding model; the binding constant for **3·6** was found to be 2300 M^{-1} and that for **3·7** was determined to be 4100 M^{-1}.

The spectral changes observed during the titrations of the receptor **4**, including the 1-imidazolyl unit, with β-glucopyranoside **5** (see Figure S4 in the Supporting Information and Figure 13b and c) are less substantial than those observed during the titrations of **1** with **5**. The spectroscopic changes indicated 1:1 binding followed by an association of the second sugar molecule (mixed 1:1 and 1:2 receptor–sugar binding model; this is a different binding model as that determined for the complexation of **1** with **5**). The binding constants for **4·5** were found to be 3560 M^{-1} (K_{11}) and 1300 M^{-1} (K_{12}; $\beta_{12}=4.87\times10^6\,M^{-2}$). Thus, the interactions between **4** and **5** are significantly weaker than those observed with the receptors **1** and **2**.

Conclusion

The analysis of the binding motifs in the protein–carbohydrate complexes (for examples, see Figure 1) has inspired the design of receptors that include suitable substituted imidazole or indole units, which represent the entities used in nature, and 2-aminopyridine groups, which act as heterocyclic analogues of the asparagine/glutamine primary amide side chains (in analogy to the binding motifs shown in Figure 1a). The recognition units are interconnected by a phenyl spacer, which was incorporated into the receptor structure to provide additional apolar contacts to a saccharide; similar to sugar-binding proteins, which commonly place aromatic surfaces against patches of sugar CH groups (see Figure 1d). The amine NH^D from the -CH_2NHCH_2- linker provides an additional hydrogen-bonding site for the binding of carbohydrates (see also reference [3i]), as is also indicated by molecular modelling (Table 2). The compounds **1** and **2** have been established as highly effective receptors for β-glucopyranoside **5**, β-maltoside **8** and α-maltoside **9**, showing 1:1 and 2:1 receptor–substrate complexation behaviour toward the carbohydrates. These receptors are able to bind the selected carbohydrates with an overall binding constant β_{21} of $10^9\,M^{-2}$ in chloroform solutions (with K_{11} and K_{21} of 10^5 and 10^3–$10^4\,M^{-1}$, respectively; see Table 1). Both hydrogen bonding and interactions of the carbohydrate CH units with the phenyl rings of the receptors contribute to the stabilisation of the 1:1 and 2:1 receptor–carbohydrate complexes. Furthermore, the receptors **1** and **2** display remarkable β- versus α-anomer selectivity in the recognition of glucopyranosides as well as epimer selectivity in the recognition of β-glucopyranoside and -galactopyranoside (see Table 1).

The formation of receptor–sugar complexes has been characterised by ^{1}H NMR spectroscopy and confirmed by a second, independent technique, namely fluorescence spectroscopy. The ^{1}H NMR titration experiments were carried out by adding increasing amounts of the corresponding mono- or disaccharide to a $CDCl_3$ solution of the receptor **1** or **2**. In addition, inverse titrations were performed in which the concentration of the monosaccharide was held constant and that of the receptor was varied. The association constants obtained on the basis of these titrations are identical, within the limits of uncertainty, to those determined from titrations in which the role of the receptor and substrate was reversed. The very high values of the binding constants for **1·5**, **2·5**, **1·8**, **2·8** and **2·9** determined on the basis of the ^{1}H NMR spectroscopic titrations[16] were fully confirmed by the fluorescence titrations in $CHCl_3$.

A significant feature observed during the titrations of β-glucopyranoside **5** with **1** or **2** (inverse titrations) was the upfield shifts of the CH signals of **5**, particularly the strong complexation-induced shift of the 2-CH proton (1.5 and 1.7 ppm for the titration with **1** and **2**, respectively). These complexation-induced chemical-shift changes are significantly larger than those usually reported for the CH protons of β-glucopyranoside in the literature. The results of the NMR spectroscopic titrations indicate the participation of the sugar CH units in the CH···π interactions with the phenyl ring of the receptor. The formation of these interactions was also suggested by molecular-modelling calculations (for examples of binding motifs indicated by molecular modelling, see Table 2). The character of carbohydrate–aromatic interactions is still a subject of controversy;[7,18] thus, the studies

with suitable model systems provide important insights on the origin of the carbohydrate–aromatic interactions.

Comparative binding studies showed that the replacement of the 4(5)-imidazolyl unit by a 2-pyrrolyl group (compound **3**) does not reduce the binding affinity of the receptor, indicating a less important contribution of the imidazole 3-N of **1** to the stabilisation of the complex **1·5** (as also indicated by molecular modelling, see Figure 8). In contrast, the incorporation of a 1-imidazolyl unit into the receptor structure (compound **4**) causes both the change of the binding model and a substantial drop in the binding affinity. Similar to the receptors **1** and **2**, the receptor **3** shows much higher affinity for the β-glucopyranoside **5** than for the α-glucopyranoside **6** and β-galactopyranoside **7** (see Table 1).

The binding studies show that the mimicking of the binding motifs found in the crystal structures of protein–carbohydrate complexes (by using natural recognition groups or their analogues) represents a powerful strategy for the design of effective and selective carbohydrate receptors. The binding of sugars with artificial receptors in a medium with a lower dielectric constant (see also reference [8]) provides important information about the factors that contribute to the affinity between receptors and saccharides and offers an important screen for effective recognition motifs for carbohydrates. The simple acyclic structure of **1**–**4** gives the possibility of an easy variation of the receptor structure, providing a base for systematic studies towards recognition motifs for carbohydrates.

Experimental Section

Analytical TLC was carried out on silica gel 60 F_{254} plates with ethyl acetate/toluene (3:1 v/v) or chloroform/methanol (7:1 v/v) as the mobile phase. Melting points are uncorrected. Octyl β-D-glucopyranoside (**5**), octyl α-D-glucopyranoside (**6**), octyl β-D-glucopyranoside (**7**), dodecyl β-D-maltoside (**8**) and dodecyl α-D-maltoside (**9**) are commercially available.

1-Bromomethyl-3,5-bis[(4,6-dimethylpyridin-2-yl)aminomethyl]-2,4,6-triethylbenzene (11): A solution of 2-amino-4,6-dimethyl-pyridine (3.16 g, 25.69 mmol) in CH_3CN (10 mL) was added to a mixture of 1,3,5-tris(bromomethyl)-2,4,6-triethyl-benzene (6.00 g, 13.60 mmol) and K_2CO_3 (3.76 g, 27.20 mmol) in CH_3CN/THF (1:1 v/v; 40 mL). The mixture was stirred at room temperature for 48 h. After filtration and evaporation of the solvents, the crude product was purified by column chromatography (ethyl acetate/toluene, 1:3 v/v). Yield: 30%; m.p. 78–79°C; ^{1}H NMR (400 MHz, $CDCl_3$): δ = 1.22 (t, J = 7.5 Hz, 3H), 1.29 (t, J = 7.5 Hz, 6H), 2.24 (s, 6H), 2.36 (s, 6H), 2.73 (q, J = 7.5 Hz, 2H), 2.85 (q, J = 7.5 Hz, 4H), 4.23 (brs, 2H), 4.37 (d, J = 4.2 Hz, 4H,), 4.62 (s, 2H), 6.10 (s, 2H), 6.35 ppm (s, 2H); ^{13}C NMR (100 MHz, $CDCl_3$) δ = 16.4, 16.7, 21.1, 22.8, 23.0, 24.1, 29.6, 40.5, 103.6, 113.9, 131.9, 133.4, 143.8, 144.9, 148.9, 156.5, 158.0 ppm; HRMS (EI): m/z: calcd for $C_{29}H_{39}BrN_4$: 522.2353; found: 522.2360; R_f = 0.12 (ethyl acetate/toluene, 1:3 v/v).

1-Aminomethyl-3,5-bis[(4,6-dimethylpyridin-2-yl)aminomethyl]-2,4,6-triethylbenzene (12): An aqueous ammonia solution (25%, 25 mL) was added to a solution of **11** (776 mg, 1.48 mmol) in THF/MeOH (1:1, *v*/*v*, 20 mL). This mixture was stirred at room temperature for 12 h. After evaporation of the solvents, water (20 mL) was added and the solution was extracted with $CHCl_3$ (3×20 mL). The combined organic phases were washed with brine (20 mL), dried over $MgSO_4$ and the solvent was removed under reduced pressure. The crude product was purified by column chromatography ($CHCl_3$/MeOH, 7:1 v/v). Yield: 72%; m.p. 82–83°C; ^{1}H NMR (300 MHz, [D_6]DMSO) δ = 1.22 (t, J = 7.3 Hz, 3H), 1.23 (t, J = 7.4 Hz, 6H), 2.23 (s, 6H), 2.36 (s, 6H), 2.72 (q, J = 7.3 Hz, 2H), 2.80 (q, J = 7.4 Hz, 4H), 3.92 (s, 2H), 4.36 (s, 6H), 6.10 (s, 2H), 6.34 ppm (s, 2H); ^{13}C NMR (100 MHz, $CDCl_3$) δ = 16.76, 16.81, 21.15, 22.48, 22.76, 23.97, 39.47, 40.63, 103.61, 113.82, 133.15, 135.02, 142.07, 142.60, 155.22, 158.27 ppm; HRMS (EI): m/z: calcd for $C_{29}H_{41}N_5$: 459.3362; found 459.3352; R_f = 0.17 ($CHCl_3$/CH_3OH 7:1 v/v).

General procedure for the synthesis of compounds 1–3: The carbaldehyde (4(5)-imidazole-, 3-indole- or 2-pyrrole-carbaldehyde; 0.76 mmol) was dissolved in methanol (5 mL) and added to a solution of compound **12** (0.76 mmol) in methanol (20 mL). The reaction mixture was stirred for 12 h. The solution was cooled to 0°C and $NaBH_4$ (0.76 mmol) was added. The reaction mixture was then stirred for 1 h at 0°C and for an additional 2 h at room temperature. The solvent was removed and the residue taken up in chloroform/water (20 mL, 1:1) The aqueous phase was washed twice with chloroform and the combined organic phases were dried over magnesium sulfate and the solvent was removed. The crude product was purified by column chromatography ($CHCl_3$/CH_3OH 5:1 or 7:1 v/v).

1-[(4-Imidazolyl-methyl)aminomethyl]-3,5-bis[(4,6-dimethylpyridin-2-yl)aminomethyl]-2,4,6-triethylbenzene (1): Yield: 32%; m.p. 103–104°C; ^{1}H NMR (400 MHz, $CDCl_3$) δ = 1.13 (t, J = 7.5 Hz, 6H), 1.19 (t, J = 7.5 Hz, 3H), 2.21 (s, 6H), 2.33 (s, 6H), 2.68 (q, J = 7.5 Hz, 6H), 3.75 (s, 2H), 3.87 (s, 2H), 4.31 (s, 4H), 4.40 (brs, 2H), 6.10 (s, 2H), 6.32 (s, 2H), 6.89 (d, J = 0.6 Hz, 1H), 7.40 ppm (d, J = 0.6 Hz, 1H); ^{13}C NMR (100 MHz, $CDCl_3$) δ = 16.68, 16.71, 21.03, 22.66, 22.76, 23.92, 40.53, 46.03, 46.42, 103.61, 113.78, 118.65 135.28, 132.63, 133.87, 142.96, 143.18, 148.92, 156.27, 158.14 ppm; HRMS (ESI): m/z: calcd for $C_{33}H_{46}N_7$: 540.3809; found 540.3804; R_f = 0.06 ($CHCl_3$/CH_3OH, 7:1 v/v).

1-[(3-Indolylmethyl)aminomethyl]-3,5-bis[(4,6-dimethylpyridin-2-yl)aminomethyl]-2,4,6-triethylbenzene (2): Yield: 36%; m. p. 97–98°C; ^{1}H NMR (400 MHz, $CDCl_3$) δ = 1.09 (t, J = 7.5 Hz, 6H), 1.17 (t, J = 7.5 Hz, 3H), 2.18 (s, 6H), 2.34 (s, 6H), 2.67 (q, J = 7.5 Hz, 6H), 3.82 (s, 2H), 4.11 (s, 2H), 4.22 (brs, 2H), 4.32 (d, J = 3.8 Hz, 4H), 6.01 (s, 2H), 6.31 (s, 2H), 7.13 (m, 3H), 7.30 (d, J = 8.0 Hz, 1H), 7.68 (d, J = 8.0 Hz, 1H), 8.44 ppm (brs, 1H); ^{13}C NMR (100 MHz, $CDCl_3$) δ = 16.70, 16.79, 21.04, 22.76, 22.82, 24.13, 40.55, 45.11, 46.89, 103.74, 111.14, 113.70, 118.84, 119.62, 122.09, 125.07, 127.19, 128.23, 132.77, 136.35, 143.05, 143.34, 148.70, 156.48, 158.20 ppm; HRMS (ESI): m/z: calcd for $C_{38}H_{48}N_6$: 589.4013; found 589.4014; R_f = 0.09 ($CHCl_3$/CH_3OH 7:1 v/v).

1-[(2-Pyrrolylmethyl)aminomethyl]-3,5-bis[(4,6-dimethylpyridin-2-yl)aminomethyl]-2,4,6-triethylbenzene (3): Yield: 42%; m.p. 79–80°C; ^{1}H NMR (400 MHz, $CDCl_3$) δ = 1.16 (t, J = 7.5 Hz, 6H), 1.19 (t, J = 7.4 Hz, 3H), 2.21 (s, 6H), 2.34 (s, 6H), 2.68 (q, J = 7.4 Hz, 2H), 2.69 (q, J = 7.5 Hz, 4H), 3.75 (s, 2H), 3.89 (s, 2H), 4.24 (brs, 2H), 4.34 (d, J = 4.1 Hz, 4H), 6.07 (s, 2H), 6.11 (m, 2H), 6.33 (s, 2H), 6.68 (m, 1H), 8.86 ppm (brs, 1H); ^{13}C NMR (100 MHz, $CDCl_3$) δ = 16.76, 16.80, 21.05, 22.78, 22.85, 24.11, 40.56, 46.45, 46.87, 103.57, 106.94, 108.04, 113.78, 117.57, 130.13, 132.91, 143.18, 143.25, 148.72, 156.55, 158.20 ppm; HRMS (EI): m/z: calcd for $C_{34}H_{46}N_6$: 538.3778; found 538.3780; R_f = 0.11 ($CHCl_3$/CH_3OH 7:1 v/v).

1-[(1-Imidazolyl)methyl]-3,5-bis[(4,6-dimethylpyridin-2-yl)aminomethyl]-2,4,6-triethylbenzene (4): A solution of compound **11** (500 mg, 0.96 mmol) in THF (10 mL) was added dropwise to a mixture of imidazole (65 mg, 0.96 mmol) and K_2CO_3 (132 mg, 0.96 mmol) in THF (20 mL). The mixture was stirred at room temperature for 24 h. After filtration and evaporation of solvents, the crude product was purified by column chromatography (silica gel, chloroform/methanol 20:1 and 7:1 v/v). Yield: 30%; m.p. 68–69°C; ^{1}H NMR (400 MHz, $CDCl_3$) δ = 1.12 (t, J = 7.5 Hz, 6H), 1.25 (t, J = 7.5 Hz, 3H), 2.23 (s, 6H), 2.35 (s, 6H), 2.69 (q, J = 7.5 Hz, 4H), 2.77 (q, J = 7.5 Hz, 2H), 4.20 (t, J = 4.0 Hz, 2H), 4.39 (d, J = 4.0 Hz, 4H), 5.18 (s, 2H), 6.10 (s, 2H), 6.35 (s, 2H), 6.75 (t, J = 1.1 Hz, 1H), 7.02 (t, J = 1.1 Hz, 1H), 7.39 ppm (s, 1H); ^{13}C NMR (100 MHz, $CDCl_3$) δ = 16.09, 16.70, 21.02, 22.93, 24.09, 40.44, 44.66, 103.46, 114.00, 118.55 128.74, 129.30, 133.69, 136.41, 143.79, 145.07, 148.77, 156.64, 158.01 ppm; HRMS (EI): m/z: calcd for $C_{32}H_{42}N_6$: 510.3465; found 510.3466; R_f = 0.32 ($CHCl_3$/CH_3OH 7:1 v/v).

CCDC-663894 contains the supplementary crystallographic data for this paper. These data can be obtained free of charge from The Cambridge Crystallographic Data Centre via www.ccdc.cam.ac.uk/data_request/cif.

Supporting information for this article is available on the WWW under http://www.chemeurj.org/ or from the author and contains ^{1}H und ^{13}C NMR spectra of compounds **1**–**4**, IR data of compounds **1**–**4**, examples of ^{1}H NMR titrations of receptor **3** and **4** with β-glucopyranoside **5**, an example of ^{1}H NMR titration of β-glucopyranoside **5** with receptor **3** (inverse titration), further examples of titration curves, representative mole-ratio plots and X-ray data for compound **11**.

Acknowledgements

Financial support by the Deutsche Forschungsgemeinschaft is gratefully acknowledged. We thank Prof. Dr. Peter G. Jones (Institut für Anorganische and Analytische Chemie der Technischen Universität Braunschweig) for performing the X-ray measurements of **11**.

[1] a) F. A. Quiocho, *Pure. Appl. Chem.* **1989**, *61*, 1293–1306; b) S. P. Spurlino, G.-Y. Lu, F. A. Quiocho, *J. Biol. Chem.* **1991**, *266*, 5202–5219; c) F. A. Quiocho, D. K. Wilson, *Nature* **1989**, *340*, 404–408; d) N. K. Vyas, M. N. Vyas, F. A. Quiocho, *Science* **1988**, *242*, 1290–1295; e) R. U. Lemieux, *Chem. Soc. Rev.* **1989**, *18*, 347–374; f) W. I. Weiss, K. Drickamer, *Annu. Rev. Biochem.* **1996**, *65*, 441–473; g) H. Lis, N. Sharon, *Chem. Rev.* **1998**, *98*, 637–674; h) H. Lis, N. Sharon, *Lectins*, Kluwer, Dordrecht, **2003**; i) T. R. Transue, A. K. Smith, H. Mo, I. J. Goldstein, M. A. Saper, *Nat. Struct. Biol.* **1997**, *4*, 779–782; j) M. Cygler, D. R. Rose, D. R. Bundle, *Science* **1991**, *253*, 442–445.

[2] For reviews on carbohydrate recognition with artificial receptors, see: a) A. P. Davis, T. D. James in *Functional Synthetic Receptors*, (Eds.: T. Schrader, A. D. Hamilton), Wiley-VCH, Weinheim, **2005**, p. 45–109; b) A. P. Davis, R. S. Wareham, *Angew. Chem.* **1999**, *111*, 3161–3179; *Angew. Chem. Int. Ed.* **1999**, *38*, 2979–2996; c) *Host-Guest Chemistry - Mimetic Approaches to Study Carbohydrate Recognition* (Ed.: S. Penadés), *Top. Curr. Chem. Vol. 218*, Springer, Berlin, **2002**.

[3] For recent examples of carbohydrate receptors operating through noncovalent interactions, see: a) E. Klein, Y. Ferrand, E. K. Auty, A. P. Davis, *PhysChemComm* **2007**, 2390–2392; b) M. Mazik, H. Cavga, *J. Org. Chem.* **2007**, *72*, 831–838; c) M. Mazik, A. König, *Eur. J. Org. Chem.* **2007**, 3271–3276; d) M. Mazik, H. Cavga, *Eur. J. Org. Chem.* **2007**, 3633–3638; e) C. Schmuck, M. Heller, *Org. Biomol. Chem.* **2007**, *5*, 787–791; f) O. Francesconi, A. Ienco, G. Moneti, C. Nativi, S. Roelens, *Angew. Chem.* **2006**, *118*, 6845–6848; *Angew. Chem. Int. Ed.* **2006**, *45*, 6693–6696; g) M. Mazik, A. König, *J. Org. Chem.* **2006**, *71*, 7854–7857; h) M. Mazik, H. Cavga, *J. Org. Chem.* **2006**, *71*, 2957–2963; i) M. Mazik, M. Kuschel, W. Sicking, *Org. Lett.* **2006**, *8*, 855–858; j) M. Mazik, H. Cavga, P. G. Jones, *J. Am. Chem. Soc.* **2005**, *127*, 9045–9052; k) H. Abe, Y. Aoyagi, M. Inouye, *Org. Lett.* **2005**, *7*, 59–61; l) E. Klein, M. P. Crump, A. P. Davis, *Angew. Chem.* **2005**, *117*, 302–306; *Angew. Chem. Int. Ed.* **2005**, *44*, 298–302; m) M. G. J. ten Cate, D. N. Reinhoudt, M. Crego-Calama, *J. Org. Chem.* **2005**, *70*, 8443–8453; n) H. Abe, N. Masuda, M. Waki, M. Inouye, *J. Am. Chem. Soc.* **2005**, *127*, 16189–16196; o) J. M. Benito, M. Meldal, *QASR Comb. Sci.* **2004**, *23*, 117–129; p) G. Gupta, C. R. Lowe, *J. Mol. Recognit.* **2004**, *17*, 218–235; q) T. Velasco, G. Lecollinet, T. Ryan, A. P. Davis, *Org. Biomol. Chem.* **2004**, *2*, 645–647; r) J.-M. Fang, S. Selvi, J.-H. Liao, Z. Slanina, C.-T. Chen, P.-T. Chou, *J. Am. Chem. Soc.* **2004**, *126*, 645–647; s) M. Mazik, W. Radunz, R. Boese, *J. Org. Chem.* **2004**, *69*, 7448–7462; t) M. Mazik, W. Sicking, *Tetrahedron Lett.* **2004**, *45*, 3117–3121.

[4] a) R. Welti, Y. Abel, V. Gramlich, F. Diederich, *Helv. Chim. Acta* **2003**, *86*, 548–562; b) K. Wada, T. Mizutani, S. Kitagawa, *J. Org. Chem.* **2003**, *68*, 5123–5131; c) M. Segura, B. Bricoli, A. Casnati, E. M. Muñoz, F. Sansone, R. Ungaro, C. Vicent, *J. Org. Chem.* **2003**, *68*, 6296–6303; d) R. Welti, F. Diederich, *Helv. Chim. Acta* **2003**, *86*, 494–503; e) M. Dukh, D. Saman, K. Lang, V. Pouzar, I. Cerny, P. Drasar, V. Král, *Org. Biomol. Chem.* **2003**, *1*, 3458–3463; f) T. Ishi-I, M. A. Mateos-Timoneda, P. Timmerman, M. Crego-Calama, D. N. Reinhoudt, S. Shinkai, *Angew. Chem.* **2003**, *115*, 2402–2407; *Angew. Chem. Int. Ed.* **2003**, *42*, 2300–2305; g) G. Lecollinet, A. P. Dominey, T. Velasco, A. P. Davis, *Angew. Chem.* **2002**, *114*, 4267–4270; *Angew. Chem. Int. Ed.* **2002**, *41*, 4093–4096; h) S.-i. Tamaru, S. Shinkai, A. B. Khasanov, T. W. Bell, *Proc. Natl. Acad. Sci. USA* **2002**, *99*, 4972–4976; i) K. Ladomenou, R. P. Bonar-Law, *Chem. Commun.* **2002**, 2108–2109; j) O. Rusin, K. Lang, V. Král, *Chem. Eur. J.* **2002**, *8*, 655–663; k) M. Mazik, W. Radunz, W. Sicking, *Org. Lett.* **2002**, *4*, 4579–4582; l) J. Billing, H. Grundberg, U. J. Nilsson, *Supramol. Chem.* **2002**, *14*, 367–372; m) A. S. Droz, U. Neidlein, S. Anderson, P. Seiler, F. Diederich, *Helv. Chim. Acta* **2001**, *84*, 2243–2289; n) D. W. P. M. Löwik, C. R. Lowe, *Eur. J. Org. Chem.* **2001**, 2825–2839; o) J. M. Benito, M. Gomez-Garcia, J. L. Jimenez Blanco, C. Ortiz Mellet, J. M. Garcia Fernandez, *J. Org. Chem.* **2001**, *66*, 1366–1372; p) S.-i. Tamaru, M. Yamamoto, S. Shinkai, A. B. Khasanow, T. W. Bell, *Chem. Eur. J.* **2001**, *7*, 5270–5276; q) H. J. Kim, Y. H. Kim, J. I. Hong, *Tetrahedron Lett.* **2001**, *42*, 5049–5052; r) J. Bitta, S. Kubik, *Org. Lett.* **2001**, *3*, 2637–2640; s) M. Mazik, W. Sicking, *Chem. Eur. J.* **2001**, *7*, 664–670; t) M. Mazik, H. Bandmann, W. Sicking, *Angew. Chem.* **2000**, *112*, 562–565; *Angew. Chem. Int. Ed.* **2000**, *39*, 551–554; u) F. Eblinger, H.-J. Schneider, *Collect. Czech. Chem. Commun.* **2000**, *65*, 667–672.

[5] For examples of boronic acid based receptors that use covalent interactions for sugar binding, see: a) T. Zhang, E. V. Anslyn, *Org. Lett.* **2006**, *8*, 1649–1652; b) G. Heinrichs, M. Schellenträger, S. Kubik, *Eur. J. Org. Chem.* **2006**, 4177–4186; c) S. Jiang, J. O. Escobedo, K. K. Kim, O. Alptürk, G. K. Samoei, S. O. Fakayode, I. M. Warner, O. Rusin, R. M. Strongin, *J. Am. Chem. Soc.* **2006**, *128*, 12221–12228; d) A. T. Wright, Z. Zhong, E. V. Anslyn, *Angew. Chem.* **2005**, *117*, 2–5; *Angew. Chem. Int. Ed.* **2005**, *44*, 5679–5682; e) Z. Wang, D. Zhang, D. Zhu, *J. Org. Chem.* **2005**, *70*, 5729–5732; f) D. Stones, S. Manku, X. Lu, D. G. Hall, *Chem. Eur. J.* **2004**, *10*, 92–99; g) J. Zhao, T. M. Fyles, T. D. James, *Angew. Chem.* **2004**, *116*, 3543–3546; *Angew. Chem. Int. Ed.* **2004**, *43*, 3461–3464; h) S. Arimori, M. L. Bell, C. S. Oh, K. A. Frimat, T. D. James, *J. Chem. Soc. Perkin Trans. 1*, **2002**, 803–808; i) H. Fang, G. Kaur, B. Wang, *J. Fluorescence* **2004**, *14*, 481–489; j) H. Cao, M. H. Heagy, *J. Fluorescence* **2004**, *14*, 569–584; k) C. W. Gray, Jr., B. T. Walker, R. A. Foley, T. A. Houston, *Tetrahedron Lett.* **2003**, *44*, 3309–3312; l) M. Yamamoto, M. Takeuchi, S. Shinkai, F. Tani, Y. Naruta, *J. Chem. Soc. Perkin Trans. 2* **2000**, 9–16; m) T. Mizuno, M. Yamamoto, M. Takeuchi, S. Shinkai, *Tetrahedron* **2000**, *56*, 6193–6198; For reviews, see: n) T. D. James, S. Shinkai, *Top. Curr. Chem.* **2002**, *218*, 159–200; o) S. Striegler, *Curr. Org. Chem.* **2003**, *7*, 81–102; p) T. D. James, K. R. A. S. Sandanayake, S. Shinkai, *Angew. Chem.* **1996**, *108*, 2038–2050; *Angew. Chem. Int. Ed. Engl.* **1996**, *35*, 1910–1922.

[6] Anslyn and co-workers have exploited the 2-aminopyridine unit as a heterocyclic analogue of the asparagine/glutamine primary amide side chain for binding of cyclohexane diols and triols; C.-Y. Huang, L. A. Cabell, E. V. Anslyn, *J. Am. Chem. Soc.* **1994**, *116*, 2778–2792.

[7] For recent discussions on the importance of carbohydrate–aromatic interactions, see: a) G. Terraneo, D. Potenza, A. Canales, J. Jiménez-Barbero, K. K. Baldridge, A. Bernardi, *J. Am. Chem. Soc.* **2007**, *129*, 2890–2900; b) M. I. Chávez, C. Andreu, P. Vidal, N. Aboitiz, F. Freire, P. Groves, J. L. Asensio, G. Asensio, M. Muraki, F. J. Canada, J. Jiménez-Barbero, *Chem. Eur. J.* **2005**, *11*, 7060–7074.

[8] Many biological interactions occur in enzyme pockets or in membranes, meaning that they occur in an environment with a lower dielectric constant relative to the bulk solvent. For this reason, many theoretical studies on different enzyme model systems have been performed in a medium with a lower dielectric constant (mostly $\varepsilon = 5.7$, which corresponds to the chlorobenzene). See, for example: a) K.-B. Cho, Y. Moreau, D. Kumar, D. A. Rock, J. P. Jones, S. Shaik, *Chem. Eur. J.* **2007**, *13*, 4103–4115; b) S. P. de Visser, S. Shaik, P. K. Sharma, D. Kumar, W. Thiel, *J. Am. Chem. Soc.* **2003**,

125, 15779–15788; c) S. P. de Visser, *J. Phys. Chem. A* **2005**, *109*, 11050–11057.

[9] a) V. Král, O. Rusin, F. P. Schmidtchen, *Org. Lett.* **2001**, *3*, 873–876; b) R. D. Hubbard, S. R. Horner, B. L. Miller, *J. Am. Chem. Soc.* **2001**, *123*, 5810–5811; c) R. Yanagihara, Y. Aoyama, *Tetrahedron Lett.* **1994**, *35*, 9725–9728.

[10] C. S. Wilcox, N. M. Glagovich, Program HOSTEST 5.6, University of Pittsburgh, Pittsburgh, PA, **1994**.

[11] a) C. Frassineti, S. Ghelli, P. Gans, A. Sabatini, M. S. Moruzzi, A. Vacca, *Anal. Biochem.* **1995**, *251*, 374–382; b) P. Gans, A. Sabatini, A. Vacca, *Talanta* **1996**, *43*, 1739–1753.

[12] K. J. Wallace, R. Hanes, E. Anslyn, J. Morey, K. V. Kilway, J. Siegel, J. *Synthesis* **2005**, 2080–2083.

[13] A. R. Katritzky, A. F. Pozharski, *Handbook of Heterocyclic chemistry*, Pergamon, Amsterdam, **2000**, p. 131.

[14] a) The binding constants were determined in chloroform at 25 °C by titration experiments ($CDCl_3$ was stored over activated molecular sieves and deacidified with Al_2O_3). Dilution experiments show that receptors do not self-aggregate in the used concentration range. For each system at least three ^1H NMR titrations were carried out; for each titration 15–20 samples were prepared. b) The error in K_a was less than 10%; c) K_{11} corresponds to the 1:1 association constant. K_{21} corresponds to the 2:1 receptor–sugar association constant. K_{12} corresponds to the 1:2 receptor–sugar association constant. $\beta_{21} = K_{11} \times K_{21}$, $\beta_{12} = K_{11} \times K_{12}$.

[15] a) For each system, at least two fluorescence titrations were carried out; for each titration, 20 samples were prepared. b) The error in a single K_a estimation was less than 15%.

[16] For a discussion on limitations of the NMR method, see: L. Fielding, *Tetrahedron* **2000**, *56*, 6151–6170.

[17] For an example of macrocyclic receptor that is able to distinguish between the octyl β-D-maltoside and octyl β-D-glucopyranoside in organic media (CD_3CN/CD_3OD, 88:12 v/v), see: U. Neidlein, F. Diederich, *Chem. Commun.* **1996**, 1493–1494.

[18] For examples of CH···π interactions in the crystal structures of the complexes formed between artificial receptors and carbohydrates, see reference [3j].

Received: August 15, 2007
Published online: January 18, 2008

